ELSEVIER

Biophysical Chemistry 104 (2003) 199–208

Biophysical Chemistry

www.elsevier.com/locate/bpc

Direct voltammetry and electrochemical catalysis with horseradish peroxidase in polyacrylamide hydrogel films

Rong Huang, Naifei Hu*

Department of Chemistry, Beijing Normal University, Beijing 100875, PR China

Received 7 October 2002; received in revised form 11 November 2002; accepted 11 November 2002

Abstract

This paper reports the direct voltammetry of horseradish peroxidase (HRP) incorporated in amphiphilic polyacrylamide (PAM) films modified on pyrolytic graphite (PG) electrodes. Cyclic voltammetry of HRP-PAM films showed a pair of well-defined, nearly reversible peaks at approximately −0.33 V vs. SCE in pH 7.0 buffers, characteristic of HRP heme Fe(III)/Fe(II) redox couple. The PAM films in solution contained large amounts of water and formed a hydrogel, and provided a favorable microenvironment for HRP and facilitated its direct electron transfer with underlying PG electrodes. The apparent heterogeneous electron transfer rate constant (k_s) and formal potential ($E^{\circ\prime}$) were estimated by fitting the data of square wave voltammetry (SWV) with the non-linear regression analysis. UV-vis absorption spectra demonstrated that HRP in PAM films retained its secondary structure similar to its native state. The embedded HRP in PAM films showed the electrocatalytic activity to various substrates such as nitrite, oxygen and hydrogen peroxide. The possible mechanism of catalytic reaction of H_2O_2 with HRP-PAM films was proposed.

Keywords: Horseradish peroxidase; Polyacrylamide; Direct voltammetry; Electrochemical catalysis

1. Introduction

The investigation of direct electrochemistry of enzymes is a convenient and informative means for understanding the kinetics and thermodynamics of biological redox processes in living systems [1–3]. It also plays an important role on the development of the third generation or mediator-free biosensors [4].

Horseradish peroxidase (HRP) (EC 1.11.1.7) is one of the most intensively studied heme enzymes that catalyze the oxidation of a variety of reductants by hydrogen peroxide [5]. It contains a heme prosthetic group as its active site. The molecular weight of HRP is approximately 42 000 [5], and the isoelectric point is at pH 8.9 [6]. HRP can react with H_2O_2 to form a powerful enzymatic oxidizing agent known as Compound I, which is a two-equivalent oxidized form containing an oxyferryl heme and a porphyrin π cation radical. Compound I is catalytically active and can abstract one electron from the substrate to form a second intermediate, Compound II, which is subsequently reduced back to the resting state of the native enzyme, HRP-Fe(III), by accepting an additional electron from the substrate. HRP-Fe(III) can also be further reduced to HRP-Fe(II) [5].

*Corresponding author. Tel. +86-106-220-7838; fax: +86-106-220-0567.

E-mail address: hunaifei@bnu.edu.cn (N. Hu).

0301-4622/03/$ - see front matter
PII: S0301-4622(02)00367-8

The direct electron exchange has been reported for HRP [7]. However, most of the works on HRP electrochemistry were performed in the presence of H_2O_2 or other peroxides with amperometric technique. For example, as a biosensor, HRP immobilized on the surface of electrodes permitted amperometric measurement of H_2O_2 without using mediators. The amperometric reduction current was found to be proportional to the concentration of H_2O_2 [7–9]. This reduction current was proposed to be a reduction of Compound I or Compound II. Only a few examples of direct, quasi-reversible cyclic voltammograms (CV) of HRP were reported in the absence of H_2O_2 or other peroxides, showing the difficulty of electron transfer between the electrodes and the redox center of HRP, which is buried deeply inside the polypeptide chains.

Recently, Mazumdar and his colleague reported a pair of quasi-reversible CV peaks of HRP in pH 7.4 solutions at +0.70 V vs. NHE at pretreated indium tin oxide electrodes, attributed to Compound II/HRP-Fe(III) redox couple [10]. As for HRP Fe(III)/Fe(II) couple, Ferri et al. [11,12] reported a CV peak pair at −0.38 V vs. SCE by entrapping HRP in the film of tributylmethyl phosphonium chloride (TBMPC) polymer bound to an anionic exchange resin at pyrolytic graphite (PG) electrodes. Direct CV response of HRP Fe(III)/Fe(II) couple was also reported at didodecyldimethylammonium bromide (DDAB) [13], DNA [14], and AQ [15] film electrodes. These films provided a suitable microenvironment for HRP, and greatly enhanced the electron communication between HRP and electrodes. Electrocatalytic reduction of H_2O_2 by HRP in these films was also described. HRP immobilized on a colloidal gold modified carbon paste electrode [16] or on a colloid/cysteamine-modified gold electrode [17] also showed direct electrochemistry.

Polyacrylamide (PAM) is a kind of widely used polymers. PAM has a long hydrophobic hydrocarbon backbone with hydrophilic amide groups, showing the amphiphilic property. The electrochemistry of heme proteins in PAM polymer environment has been studied. Murray and co-workers has reported 'solid-state' voltammetry of cytochrome *c* in PAM gel solvent [18]. In the previous study, we found that PAM could form stable films on PG surface and absorb considerable amounts of water in aqueous solution. Heme proteins such as hemoglobin (Hb) [19] and myoglobin (Mb) [20] in the PAM hydrogel films modified on PG electrodes demonstrated a reversible CV response for the heme Fe(III)/Fe(II) redox couple. Since HRP is also a heme protein with similar properties to Hb and Mb in some aspects, we expect that HRP could also be incorporated in PAM films and show direct voltammetric responses. In this paper, a reversible voltammogram of HRP in PAM films was obtained for its heme Fe(III)/Fe(II) couple and HRP-PAM films were characterized by various techniques. The catalytic reduction of nitrite, oxygen and hydrogen peroxide at HRP-PAM film electrodes were also studied. The catalytic reaction of H_2O_2 at HRP-PAM film electrodes was found to be associated with the production of oxygen and further reduction of O_2.

2. Experimental

2.1. Reagents

Lyophilized HRP (RZ > 3, 250 units/mg) was from Shanghai Promega and used as received. The HRP solution of 0.2 mM in phosphate buffers at pH 7.0 was stored at 4 °C. Polyacrylamide (PAM, MW 3 000 000) was from Shanghai Reagent Company. Sodium nitrite was from Beijing Shuanghuan Chemical Company. Hydrogen peroxide (30%) was from Beijing Chemical Engineering Plant. All other chemicals were reagent grade.

The supporting electrolyte was usually 0.05 M potassium dihydrogen phosphate at pH 7.0 containing 0.1 M KCl. Other buffers were 0.1 M sodium acetate, 0.05 M boric acid or 0.05 M citric acid, all containing 0.1 M KCl. The pHs were adjusted with HCl or NaOH solutions. All solutions were prepared with twice distilled water.

2.2. Preparation of HRP-PAM films

Prior to coating, basal plane pyrolytic graphite (PG, Advanced Ceramics, geometric area 0.16 cm^2) disk electrodes were polished with metallographic sand papers (400 grit) while flushing with

water. Electrodes were then ultrasonicated in water for 20 s.

Ten microlitres of 1 mg ml^{-1} PAM in water was spread evenly onto a freshly abraded PG electrode surface with a microsyringe. A small bottle was fit tightly over the electrode to serve as a closed evaporation chamber so that water was evaporated slowly. After the films stood over night, 10 μl of 0.2 mM HRP buffer solution were added onto the dry PAM film surface. After being dried in the small chamber for over 5 h, the HRP-PAM films were further dried in air overnight.

2.3. Apparatus and procedures

A CHI 660 electrochemical workstation (CH Instruments) was used for cyclic voltammetry (CV) and square wave voltammetry (SWV). The electrochemical cell consisted of three electrodes, where a PG disk coated with films acted as working electrode, a saturated calomel electrode (SCE) as reference and a platinum flake as counter electrode. All experiments were done at ambient temperature (20 ± 2 °C). The voltammetry at electrodes coated with HRP-PAM films was done in buffers containing no HRP. Buffers were purged with purified nitrogen for 20 min prior to a series of experiments. A nitrogen environment was then maintained over solutions for exclusion of oxygen during experiments. In aerobic experiments, measured volumes of air were injected via a syringe to solutions in a sealed cell, which had been previously degassed with purified nitrogen.

The UV-vis absorption spectroscopy was done with a Cintra 10e spectrometer (GBC). Films on glass slides for spectroscopy were prepared with the similar method to that on PG electrodes for the voltammetry.

3. Results

3.1. Cyclic voltammetry (CV)

Fig. 1a shows the steady state of cyclic voltammogram of HRP-PAM films in pH 7.0 buffers. When a HRP-PAM film electrode was immersed into the buffer solution, after several CV scan cycles, a pair of well-defined, nearly reversible

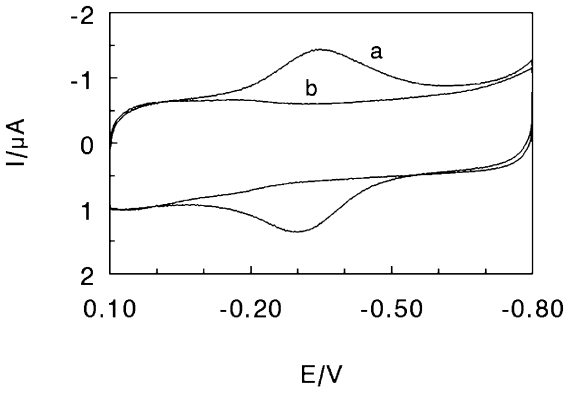

Fig. 1. Cyclic voltammograms at 0.2 V s^{-1} in pH 7.0 buffers for (a) HRP-PAM films, (b) PAM films.

peaks was observed at approximately -0.33 V vs. SCE, characteristic of Fe(III)/Fe(II) redox couple of the HRP heme prosthetic group [11,13,14]. As a control, PAM films containing no HRP showed no CV response under the same condition (Fig. 1b).

HRP-PAM films showed approximately symmetric CV peaks with nearly equal heights of the reduction and oxidation peak. The reduction peak currents were found to be linear with scan rates in the range of 0.04 to 2 V s^{-1}. Integration of reduction peaks at different scan rates gave nearly constant charge values. All these are characteristic of the surface-confined or thin-layer electrochemistry [21], suggesting that electroactive HRP-Fe(III) in the PAM films are all converted to HRP-Fe(II) on the cathodic scan, with full conversion of HRP-Fe(II) back to HRP-Fe(III) on the reverse anodic scan. Using the integrals of the reduction peaks and Faraday's law [21], the average surface concentration of electroactive HRP in the films (Γ^*) was estimated to be $(4.0 \pm 0.2) \times 10^{-11}$ mol cm^{-2}. The fraction of electroactive HRP among total deposited HRP in HRP-PAM films is only approximately 0.32%.

The film stability was tested by two methods. With the 'wet' method, an HRP-PAM film electrode was stored in pH 7.0 buffers all the time and CVs were run periodically. Alternatively, an HRP-PAM film electrode was stored in air as its dry form for most of the storing time, and CVs were

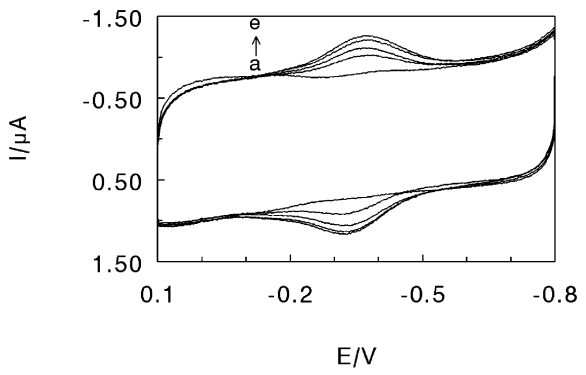

Fig. 2. Cyclic voltammograms at 0.2 V s^{-1} for PAM films immersed in pH 7.0 buffer solutions containing 0.2 mM HRP for: (a) 2 min, (b) 1 day, (c) 3 days, (d) 5 days, (e) 7 days.

tested occasionally after returning the dry films to buffers. The results of both methods showed that the peak potentials and currents of HRP-PAM films were quite stable for at least one week.

To test the possibility of HRP entering the PAM films from its solution, a PAM film electrode was placed into a pH 7.0 buffer containing HRP, and CVs were run at different soaking times (Fig. 2). The reduction peak at approximately -0.3 V grew with the immersion time, suggesting increasing amounts of HRP enter the PAM films. CVs representing films fully loaded with HRP were obtained in approximately 7 days. When fully loaded HRP-PAM films were removed from the HRP solution, and transferred to a buffer containing no HRP at the same pH, its CV response was identical to that in HRP solutions and quite stable. At the steady state, the peak potentials were similar to those of cast HRP-PAM films, but the peak heights were smaller than the latter. Since the cast method was more convenient and quantitative than the immersing method, it was used for the following studies.

The effect of pH on CV of HRP-PAM films was also examined. Results showed that an increase of pH in solution led to a negative shift in potential for both reduction and oxidation peaks for the films. The formal potential ($E^{\circ\prime}$), estimated as the midpoint of CV reduction and oxidation peak potentials for the HRP Fe(III)/Fe(II) redox couple, had a linear relationship with pH from pH 3 to 11 with a slope of -48 mV pH^{-1} (Fig. 3). This slope value is reasonably close to the theoretical value of -58 mV pH^{-1} at 20 °C for a reversible electron transfer coupled by proton transportation with the equal number of proton and electron [22,23]. Since each HRP molecule has only one heme group, this slope suggests that a single protonation accompanies the one-electron transfer of HRP-Fe(III) to electrodes. Thus, the simplified equation for the electrochemical reduction of HRP in PAM films can be expressed as

$$\text{HRP-Fe(III)} + \text{H}^+ + \text{e}^- \leftrightharpoons \text{HRP-Fe(II)}$$

3.2. Square wave voltammetry (SWV)

Square wave voltammetry (SWV), as a pulse electrochemical method [24], is easier to analyze quantitatively than the sweep method such as CV, and was used here to estimate the formal potential ($E^{\circ\prime}$) and apparent heterogeneous electron transfer rate constant (k_s). The procedure employed nonlinear regression analysis for SWV forward and reverse curves, as described in detail previously [25,26]. In brief, since the SWV model of a single electroactive species with the surface-confined electrochemical behavior [27] could not fit the experimental SWV data of the enzyme films, we combined the single-species surface-confined SWV model [27] with a formal potential ($E^{\circ\prime}$) dispersion model [25,26]. Thus, the total SWV

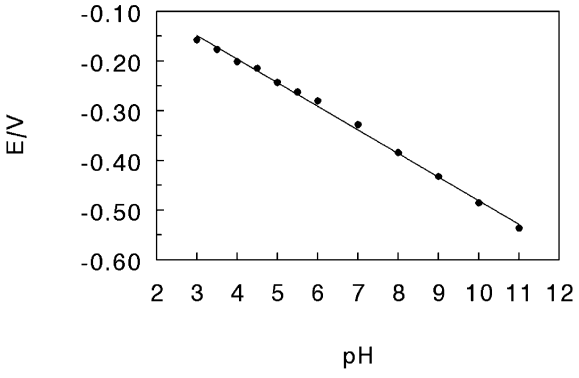

Fig. 3. Influence of pH on formal potentials for HRP-PAM films from CV at 0.2 V s^{-1}.

current (I) can be expressed as

$$I=\sum_{j=1}^{p} I_j \tag{1}$$

where I_j is the contribution of the jth of p classes of redox centers with the formal potential $E_j^{\circ\prime}$ to the total current, given by

$$I_j=(nFA\Gamma_j^*)\frac{\Psi_j}{t_p} \tag{2}$$

here, n is the number of electrons transferred per redox center, F is Faraday's constant, A is the electrode area (cm^2), Γ_j^* is the surface concentration (mol cm^{-2}) of the jth class, t_p is the pulse width, and ψ_j is the dimensionless current.

$$\Psi_j=\left[(\kappa_{f,j}+\kappa_{b,j})\Gamma'_{o,j}-\kappa_{b,j}\right]\exp\left[-(\kappa_{f,j}+\kappa_{b,j})\right] \tag{3}$$

and

$$\Gamma''_{o,j}=\frac{\Psi_j+\kappa_{b,j}}{(\kappa_{f,j}+\kappa_{b,j})} \tag{4}$$

where $\Gamma'_{o,j}$ is the jth surface concentration ratio $\Gamma_{o,j}/\Gamma_j^*$ at time $t=0$, $\Gamma'_{o,j}$ is the ratio $\Gamma_{o,j}/\Gamma_j^*$ at time $t=t_p$, $\kappa_{f,j}=k_{f,j}t_p$, $\kappa_{b,j}=k_{b,j}t_p$ and $\Gamma_{o,j}$ is the jth surface concentration for the oxidizing species. Forward and reverse dimensionless electron transfer rate constant k_f and k_b, respectively, are defined as in the Butler–Volmer equation [28]:

$$k_{f,j}=k_s t_p \exp[-\alpha(nF/\mathrm{RT})(E-E_j^{\circ\prime})] \tag{5}$$

and

$$k_{b,j}=k_s t_p \exp[(1-\alpha)(nF/\mathrm{RT})(E-E_j^{\circ\prime})] \tag{6}$$

where k_s is the apparent heterogeneous electron transfer rate constant (s^{-1}), α is the electrochemical transfer coefficient, E is the applied potential, $E_j^{\circ\prime}$ is the formal potential of the jth class of redox center. Parameters used in the fitting were average k_s, average α, the p $E_j^{\circ\prime}$ values, and the p Γ_j^* values.

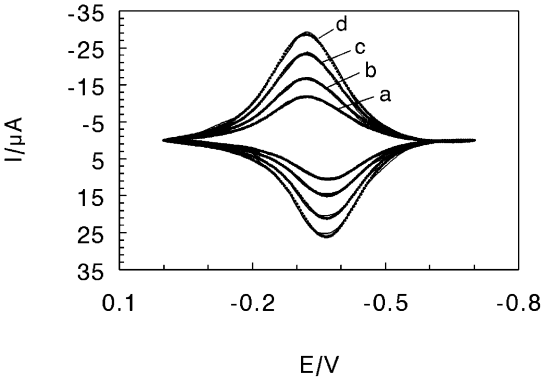

Fig. 4. Square-wave forward and reverse current voltammograms for HRP-PAM films in pH 7.0 buffers at different frequencies. Points represented the experimental SWVs from which the background had been subtracted. The solid line was the best fit by non-linear regression onto the 5-$E^{\circ\prime}$ dispersion model. SWV conditions: pulse height 60 mV, step height 4 mV, and frequencies (Hz): (a) 125; (b) 152; (c) 179; (d) 200.

Since the model ignores rate limiting ion entry or ejection, and molecular interactions within the films, it has some limitations in interpreting the apparent rate constant k_s. Any physical or chemical factors which might affect the SWV curve shape are embodied in this apparent rate constant, and k_s obtained by this method is probably best interpreted as an estimation of the rate for overall electron transfer process dependent on film and electrode properties. It is more suitable for between-film comparisons.

Preliminary studies showed that the $E^{\circ\prime}$ dispersion model with $p=5$ gave a reasonable compromise between acceptable accuracy of fit, consistency of parameters, and time of computation, and thus was used for the HRP-PAM films. The influence of different p values on the fitting results was discussed in detail by Rusling et al. [25]. The same 5-$E^{\circ\prime}$ dispersion model was also used previously for Hb-PAM [19] and HRP-AQ [15] films.

Examples of analysis of SWV data for HRP-PAM films showed goodness of fit onto the model over a range of frequencies (Fig. 4) and amplitudes. The average k_s obtained from fitting SWV data at pH 7.0 was 72 s^{-1}, and the average $E^{\circ\prime}$ was -0.321 V vs. SCE (Table 1). Parameter

Table 1
Apparent heterogeneous electron transfer rate constants and formal potentials for HRP in various films

Film[a]	pH	av. $E^{\circ\prime}/V$ (vs. SCE)		k_s, s^{-1}	Ref.[b]
		CV	SWV		
HRP-PAM	7.0	−0.331	−0.321	72±14	tw
HRP-AQ	7.0	−0.331	−0.314	42±4	[15]
HRP-DDAB	6.1	−0.150	−0.159	9.0±1.8	[13]
HRP-TBMPC	7.0	−0.377			[11]
HRP-DNA	6.1	−0.254		1.13[c]	[14]

[a] PAM = polyacrylamide, AQ = Eastman AQ, DDAB = didodecyldimethylammonium bromide, TBMPC = tributylmethyl phosphonium chloride.

[b] tw: this work, reporting average values for analysis of eight SWVs with the 5-$E^{\circ\prime}$ dispersion model at frequencies of 100–200 Hz, amplitudes of 60–75 mV, and a step height of 4 mV.

[c] by CV.

values for other HRP films are also listed in Table 1 for comparison. While the k_s values obtained by SWV in the present work and in the literatures [13,15] were all the average of eight measurements at various frequencies and amplitudes, they had different relative errors. In the estimation of k_s, HRP-AQ films showed an approximate 10% relative error, while HRP-PAM and HRP-DDAB films demonstrated relative errors of approximately 20%.

Results of regression analysis for Γ_j^* were used to plot distribution diagrams as relative amounts of redox center of electroactive protein with each of the different $E_j^{\circ\prime}$ values. Roughly Gaussian distributions were obtained.

3.3. UV-vis spectroscopy

The position of the Soret absorption band in UV-vis absorption spectra can provide information about possible denaturation of heme proteins [29], and is a useful conformational probe for the study of heme proteins, especially for the study of conformational change in the heme group region. The film cast from HRP alone gave the Soret band at 404 nm (Fig. 5a), which is the same as for the native HRP in solution at pH 7.0. HRP-PAM films cast on transparent glass slides also showed Soret band at 404 nm (Fig. 5b), suggesting that HRP in PAM films has a secondary structure similar to its native conformation.

3.4. Catalytic reduction of NO_2^-

The electrochemical reduction of nitrite could be catalyzed by HRP-PAM films (Fig. 6). When NO_2^- was added in a pH 7.0 buffer, a new catalytic reduction peak was observed at approximately −0.84 V. The peak current increased with the concentration of NO_2^-. The direct reduction of NO_2^- on plain PAM films, as well as that at bare PG electrodes, was found at the potential more negative than −1.3 V. Thus, HRP-PAM films decreased reduction overpotential of NO_2^- by at least 0.5 V. Although the mechanism of NO_2^- reduction on HRP-PAM films is not yet very clear, it is probably similar to that on myoglobin (Mb)-DDAB films [30], since Mb is also a heme protein. At Mb-DDAB film electrodes, the catalytic reduction product was confirmed to be N_2O, which was detected by mass spectroscopy on electrolysis at −0.895 V in pH 7 buffers [30].

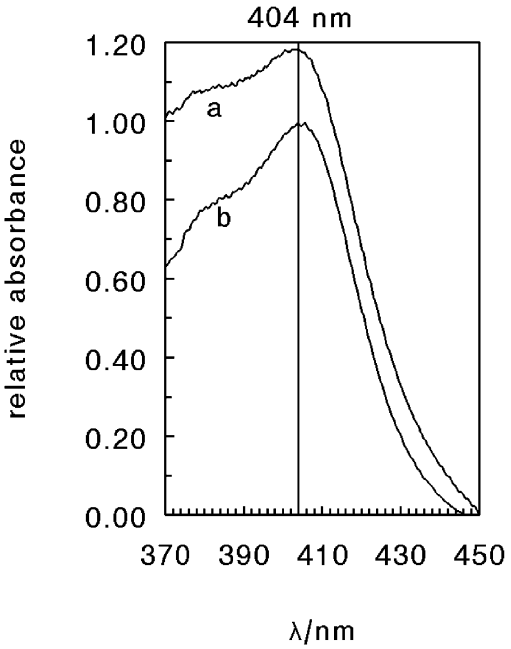

Fig. 5. UV-vis absorption spectra of (a) HRP films, (b) HRP-PAM films.

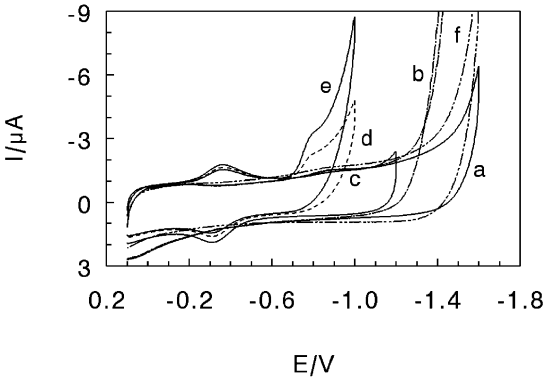

Fig. 6. Cyclic voltammograms at 0.2 V s^{-1} in pH 7.0 buffers for (a) PAM films with no $NaNO_2$ present, (b) PAM films with 0.05 M $NaNO_2$ present, (c) HRP-PAM films with no $NaNO_2$ present, (d) HRP-PAM films with 0.05 M $NaNO_2$ present, (e) HRP-PAM films with 0.12 M $NaNO_2$ present, (f) bare PG electrodes with 0.05 M $NaNO_2$ present.

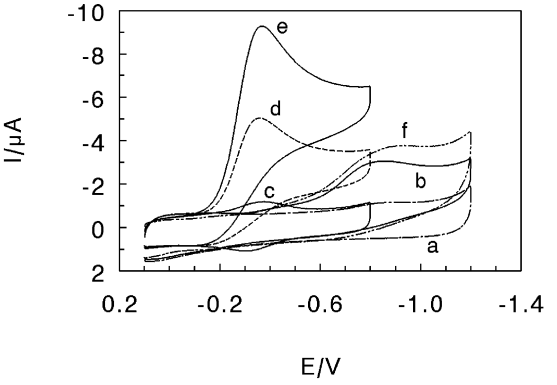

Fig. 7. Cyclic voltammograms at 0.2 V s^{-1} in 10 ml of pH 7.0 buffers for (a) PAM films with no oxygen present, (b) PAM films after 20 ml of air was injected into a sealed cell, (c) HRP-PAM films with no oxygen present, (d) HRP-PAM films after 20 ml of air was injected, (e) HRP-PAM films after 40 ml of air was injected, (f) bare PG electrodes after 20 ml of air was injected.

3.5. Catalytic reaction of O_2 and H_2O_2

HRP in PAM films had significant catalytic reactivity toward reduction of oxygen. When a certain volume of air was passed through a pH 7.0 buffer by a syringe, compared with the reduction peak of HRP-PAM films in the absence of oxygen, a great increase in reduction peak at approximately −0.36 V was observed (Fig. 7). This increase was accompanied by the disappearance of the oxidation peak of HRP-Fe(II) because HRP-Fe(II) had reacted with oxygen. The reduction peak current increased with the amount of oxygen in solution. For PAM films with no HRP incorporated, the peak for the direct reduction of oxygen was observed at approximately −0.8 V, while for bare PG electrodes, the reduction peak of oxygen was at −0.9 V. Thus, HRP-PAM films decreased the reduction overpotential of oxygen by at least 0.4 V. The ratio of reduction peak currents in the presence (I_c) and in the absence (I_d) of oxygen, I_c/I_d, decreased with increasing the scan rate (Fig. 8), also characteristic of electrochemical catalysis [31].

Electrocatalytic reduction of hydrogen peroxide was also observed by HRP-PAM films (Fig. 9). When H_2O_2 was added to a pH 7.0 buffer, an increase in reduction peak at approximately −0.36 V was seen with the disappearance of oxidation peak for HRP-Fe(II). The reduction peak current increased with the concentration of H_2O_2 in solution. However, little evidence of direct reduction of H_2O_2 was observed at bare PG or blank PAM film electrodes.

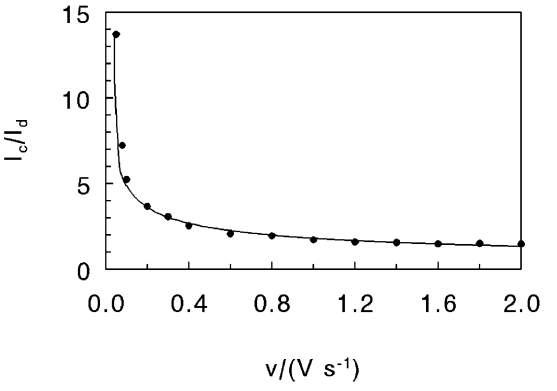

Fig. 8. Influence of scan rates on the peak current ratio, i_c/i_d, for HRP-PAM films in 10 ml of pH 7.0 buffers. i_c is the CV reduction peak current after 20 ml of air was injected into a sealed cell, i_d is the reduction peak current in the absence of oxygen.

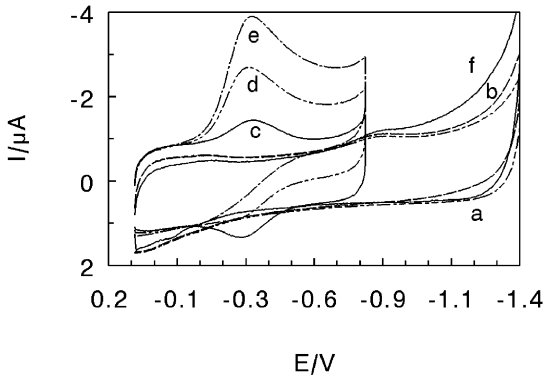

Fig. 9. Cyclic voltammograms at 0.2 V s^{-1} in pH 7.0 buffers for (a) PAM films with no H_2O_2 present, (b) PAM films with 3.5×10^{-5} M H_2O_2 present, (c) HRP-PAM films with no H_2O_2 present, (d) HRP-PAM films with 3.5×10^{-5} M H_2O_2 present, (e) HRP-PAM films with 7×10^{-5} M H_2O_2 present, (f) bare PG electrodes with 3.5×10^{-5} M H_2O_2 present.

4. Discussion

4.1. Electrochemical property

A pair of nearly reversible CV peaks of HRP heme Fe(III)/Fe(II) redox couple was observed for HRP-PAM films in buffers (Fig. 1), suggesting the direct electron transfer between HRP and PG electrodes in PAM films. The PAM films could take up HRP from its solution at pH 7.0 (Fig. 2). These results cannot be explained by Coulombic attraction as in the situation of HRP-AQ film system [15]. At pH 7.0, with its isoelectric point at pH 8.9 [6], HRP shows positive surface charges, while PAM is essentially neutral on the whole with no extra surface charges. Thus, the driving force for HRP to enter PAM films would be mainly hydrophobic interaction between the macromolecule HRP and PAM films, in which the long hydrocarbon backbone constitutes the hydrophobic region of the films. This hydrophobic interaction would also be mainly responsible for the retention of HRP in the films and the good stability for HRP-PAM films in blank buffers. The process of taking up HRP into PAM films was very slow (Fig. 2). The time required to reach the steady state was approximately 7 days. While the charge transportation involving HRP within PAM films is likely to depend on both physical diffusion and electron self-exchange, considering the slow diffusion of HRP in PAM films, electron self-exchange or 'electron hopping' may mainly contributes to the charge transport for HRP-PAM films.

The electron transfer was much faster for HRP-PAM films in blank buffers than that for HRP in solution on bare PG, on which little evidence of CV response was observed. Thus, PAM films must have a great effect on the electron transfer kinetics for HRP and provide a favorable microenvironment for its direct electrochemistry. Although the exact nature of the effect is not very clear, the PAM films may act similarly to surfactant layers on electrodes, which inhibit adsorption and/or denaturation of proteins which might otherwise block electron transfer [32]. The direct voltammetry of HRP in PAM films might also be associated with the high water content of PAM films. The formation of hydrogel films of PAM in aqueous solutions [19] may provide a more suitable microenvironment for HRP, and HRP may take a more favorable orientation in PAM films and transfer electrons with underlying PG electrodes more easily. However, only a very small fraction of HRP in the films demonstrated electroactive, suggesting that PAM hydrogel films can only enhance the electron transfer for small parts of HRP in the films, most probably those in the inner layers of the films closest to the electrode surface as other cast protein films showed [33,34].

It is well known that water has a key influence on the structure and property of PAM by the hydrogen-bond interaction between the hydrophilic amide groups of PAM and water molecules. The absorption of water by dry PAM films caused an extreme expansion of the volume and the formation of polyacrylamide hydrogel. Fully hydrated PAM films had water content of approximately 95% in the presence and absence of proteins [19,20]. This may provide a more loosening structure and a mainly aqueous microenvironment for HRP, and facilitate its electron transfer with underlying PG electrodes. The large water content of PAM films may also partially explain the capability of PAM films to take up HRP from its solution.

From fitting the surface-confined $E^{\circ\prime}$ dispersion model to the SWV data, we found that the average apparent electron transfer rate constant, k_s, for HRP in PAM films was in the same magnitude of order as in AQ films but higher than those in DDAB and DNA films (Table 1). The formal potential ($E^{\circ\prime}$) of the heme Fe(III)/Fe(II) couples of HRP-PAM films was very similar to that of HRP in AQ films but more negative than that in DNA and DDAB films, and more positive than that in TBMPC films. This confirms a specific influence of the film environment on the $E^{\circ\prime}$ of heme proteins, which had been reported previously [25,26]. Film components may change potentials via interactions with the protein or by their effect on the electrode double-layer [25,26].

4.2. Catalytic reactivity

Voltammetric data for HRP-PAM films in the presence of oxygen (Fig. 7) suggest electrochemical catalytic reduction of oxygen at the potential of the HRP Fe(III)/Fe(II) redox couple, as observed previously in HRP-AQ [15] and Mb-DDAB [35] films, as well as on bare PG electrodes in aqueous buffers and in microemulsion containing Mb [36]. In the latter work, electrochemical reduction of Mb-Fe(III) to Mb-Fe(II) occurred at the electrode, followed by a fast reaction of Mb-Fe(II) with oxygen. Mb is an oxygen carrier in biological systems and has a strong affinity for oxygen, with a rate constant of $2\times10^7\ M^{-1}\ s^{-1}$ for the formation of Mb-Fe(II)$-O_2$ at neutral pH [37]. Mb-Fe(II)$-O_2$ can then undergo an electrochemical reduction at the potential of Mb-Fe(III) reduction, producing hydrogen peroxide and Mb-Fe(II) again [36]. While the mechanism of catalytic reduction of oxygen at HRP-PAM film electrodes is not yet very clear, similar CV results to the Mb solution work might be elucidated by the pathway suggested above.

With HRP-PAM films, the catalytic reduction peak potential for hydrogen peroxide was almost the same as that for oxygen (Figs. 7 and 9), indicating the similarity of mechanism between the two systems. Reactions of hydrogen peroxide with HRP can produce Compound I [38], which is a two-oxidation equivalent higher than the native

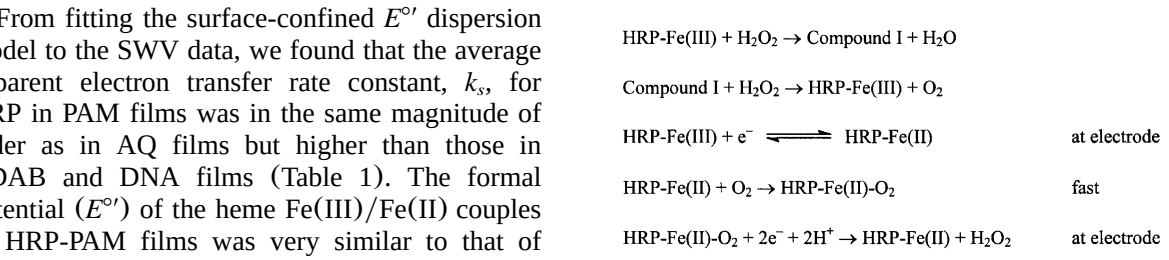

Scheme 1. Reaction mechanism of H_2O_2 with HRP.

HRP-Fe(III), often considered to be a radical $Fe^{IV}=O^{\bullet}$ species. One electron reduction of this species gives a non-radical $Fe^{IV}=O$ species known as Compound II. It was reported by spectroelectrochemistry that the reduction potentials of Compound I/Compound II and Compound II/HRP-Fe(III) couples would be at approximately 0.5–0.7 V vs. SCE [7,10,39]. Thus, it seems impossible that the catalytic CV reduction peaks at -0.36 V in Fig. 9 for HRP-PAM films in the presence of H_2O_2 result only from the electrochemical reduction of Compound I or Compound II. With excess hydrogen peroxide, the HRP/H_2O_2 system behaves as catalase [40,41]. The catalase-like reaction involves a two-electron dismutation of H_2O_2 to dioxygen and water, where H_2O_2 acts either as an oxidant or as a reductant. Compound I can be reduced by H_2O_2 through a two-electron transfer pathway and produce HRP-Fe(III) and O_2 [40,41]. The product O_2 could then be reduced catalytically at HRP-PAM film electrodes at -0.36 V with the same mechanism as proposed above for oxygen. It is the production of O_2 in the HRP/H_2O_2 system that may make the electrocatalytic CV behavior of H_2O_2 similar to that of O_2 at HRP-PAM film electrodes. A similar mechanism has been suggested for HRP in AQ [15] and lipid [42] films. Thus, a possible mechanism of electrode reaction of hydrogen peroxide catalyzed by HRP in PAM films is postulated as Scheme 1. Since no dioxygen was produced on plain PAM films in the studied potential window, the direct reduction of H_2O_2 at PAM film electrodes was not observed (Fig. 9b).

5. Conclusions

Enhanced electron transfer for the heme Fe(III)/

Fe(II) redox couple of horseradish peroxidase with pyrolytic graphite electrodes was realized in stable polyacrylamide hydrogel films. Apparent rate constant (k_s) of HRP was estimated to be 72 s^{-1} by square wave voltammetry with the aid of nonlinear regression. The HRP-PAM films are presumably stabilized mainly by hydrophobic interactions between the enzyme and polymer. HRP incorporated in PAM films essentially retained its native structure. HRP-PAM films on electrodes could catalyze reduction of nitrite, oxygen and hydrogen peroxide. The 'catalase type' mechanism was proposed for the catalytic reaction of H_2O_2 at HRP-PAM film electrodes. This HRP-PAM film electrode may have a potential application in fabricating mediator-free biosensors and bioreactors.

Acknowledgments

The financial support of the National Natural Science Foundation of China (29975003) is acknowledged.

References

[1] R.A. Marcus, N. Sutin, Biochim. Biophys. Acta 811 (1985) 265.
[2] H.B. Gray, B. Malmstrom, Biochemistry 28 (1989) 7499.
[3] G. Dryhurst, K.M. Kadish, F. Scheller, R. Rennerberg, Biological Electrochemistry, Academic Press, New York, 1982.
[4] L. Gorton, A. Lindgren, T. Larsson, F.D. Munteanu, T. Ruzgas, I. Gazaryan, Anal. Chim. Acta 400 (1999) 91.
[5] H.B. Dunford, in: J. Everse, K.E. Everse, M.B. Grisham (Eds.), Peroxidases in Chemistry and Biology, CRC press, Boca Raton, FL, 1991, p. 1.
[6] K.G. Welinder, Eur. J. Biochem. 96 (1979) 483.
[7] T. Ruzgas, E. Csoregi, J. Emneus, L. Gorton, G. Marko-Varga, Anal. Chim. Acta 330 (1996) 123.
[8] F.A. Armstrong, H.A.O. Hill, N.J. Walton, Acc. Chem. Res. 21 (1998) 407.
[9] A. Lindgren, F.D. Munteanu, I.G. Gazaryan, T. Ruzgas, L. Gorton, J. Electroanal. Chem. 458 (1998) 113.
[10] K. Chattopadhyay, S. Mazumdar, New J. Chem. 23 (1999) 137.
[11] T. Ferri, A. Poscia, R. Santucci, Bioelectrochem. Bioenerg. 44 (1998) 177.
[12] T. Ferri, A. Poscia, R. Santucci, Bioelectrochem. Bioenerg. 45 (1998) 221.
[13] X. Chen, X. Peng, J. Kong, J. Deng, J. Electroanal. Chem. 480 (2000) 26.
[14] X. Chen, C. Ruan, J. Kong, J. Deng, Anal. Chim. Acta 412 (2000) 89.
[15] R. Huang, N. Hu, Bioelectrochemistry 54 (2001) 75.
[16] S.Q. Liu, H.X. Ju, Anal. Biochem. 307 (2002) 110.
[17] Y. Xiao, H.X. Ju, H.Y. Chen, Anal. Biochem. 278 (2000) 22.
[18] B.N. Oliver, J.O. Efekeze, R.W. Murray, J. Am. Chem. Soc. 110 (1988) 2321.
[19] H. Su, N. Hu, H. Ma, Electroanalysis 12 (2000) 1064.
[20] L. Shen, R. Huang, N. Hu, Talanta 56 (2002) 1131.
[21] R.W. Murray, in: A.J. Bard (Ed.), Electroanalytical Chemistry, 13, Marcel Dekker, New York, 1984, p. 191.
[22] L. Meites, Polarographic Techniques, 2nd edition, Wiley, New York, 1965.
[23] A.M. Bond, Modern Polarographic Methods in Analytical Chemistry, Marcel Dekker, New York, 1980.
[24] J.G. Osteryoung, J.J. O'Dea, in: A.J. Bard (Ed.), Electroanalytical Chemistry, 14, Marcel Dekker, New York, 1986, p. 209.
[25] Z. Zhang, J.F. Rusling, Biophys. Chem. 63 (1997) 133.
[26] A.-E.F. Nassar, Z. Zhang, N. Hu, J.F. Rusling, T.F. Kumosinski, J. Phys. Chem. 101 (1997) 2224.
[27] J.J. O'Dea, J.G. Osteryoung, Anal. Chem. 65 (1993) 3090.
[28] A.J. Bard, L.R. Faulkner, Electrochemical Methods, Wiley, New York, 1980.
[29] P. George, G.I.H. Hanania, Biochem. J. 55 (1953) 236.
[30] R. Lin, M. Bayachou, J. Greaves, P.J. Farmer, J. Am. Chem. Soc. 119 (1997) 12689.
[31] C.P. Andrienx, C.P. Blocman, J.-M. Dumas-Bouchiat, F. M'Halla, J.M. Saveant, J. Electroanal. Chem. 113 (1980) 19.
[32] A.-E.F. Nassar, W.S. Willis, J.F. Rusling, Anal. Chem. 67 (1995) 2386.
[33] Y. Zhou, N. Hu, Y. Zeng, J.F. Rusling, Langmuir 18 (2002) 211.
[34] H. Huang, N. Hu, Y. Zeng, G. Zhou, Anal. Biochem. 308 (2002) 141.
[35] A.C. Onuoha, J.F. Rusling, Langmuir 11 (1995) 3296.
[36] A.C. Onuoha, X. Zu, J.F. Rusling, J. Am. Chem. Soc. 119 (1997) 3979.
[37] T. Wazawa, A. Matsuoka, G. Tajima, Y. Sugawara, K. Nakamura, K. Shikama, Biophys. J. 63 (1992) 544.
[38] H.B. Dunford, Peroxidases in, in: J. Everse, K.E. Everse, M.B. Grisham (Eds.), Chemistry and Biology, CRC press, Boca Raton, FL, 1991, p. 1.
[39] Z.S. Farhangrazi, M.E. Fossett, L.S. Powers, W.R. Ellis, Biochemistry 34 (1995) 2866.
[40] R. Nakajima, I. Yamazaki, J. Biol. Chem. 262 (1987) 2576.
[41] M.B. Arnao, M. Acosta, J.A. Del-Rio, R. Varon, F. Garcia-Canovas, Biochim. Biophys. Acta 43 (1990) 1041.
[42] Z. Zhang, S. Chouchane, R.S. Magliozzo, J.F. Rusling, Anal. Chem. 74 (2002) 163.